

Effect of High Energy Milling Time of the Aluminum Bronze Alloy Obtained by Powder Metallurgy with Niobium Carbide Addition

Alexandre Nogueira Ottoboni Dias ^{a*}, Aline da Silva ^a, Carlos Alberto Rodrigues ^b, Mirian de Lourdes Noronha Motta Melo ^b, Geovani Rodrigues ^b, Gilbert Silva ^b

^a Instituto de Ciências Exatas – ICE, Universidade Federal de Itajubá – UNIFEI, Av. BPS, 1303, CEP 37500-903, Itajubá, MG, Brasil

^b Instituto de Mecânica – IEM, Universidade Federal de Itajubá – UNIFEI, Av. BPS, 1303, CEP 37500-903, Itajubá, MG, Brasil

Received: April 05, 2016; Revised: February 19, 2017; Accepted: March 12, 2017

The aluminum bronze alloy is part of a class of highly reliable materials due to high mechanical strength and corrosion resistance being used in the aerospace and shipbuilding industry. It's machined to produce parts and after its use cycle, it's discarded, but third process is considered expensive and besides not being correct for environment reasons. Thus, reusing this material through the powder metallurgy (PM) route is considered advantageous. The aluminum bronze chips were submitted to high energy ball milling process with 3% of niobium carbide (NbC) addition. The NbC is a metal-ceramic composite with a ductile-brittle behaviour. It was analyzed the morphology of powders by scanning electron microscopy as well as particle size it was determined. X ray diffraction identified the phases and the influence of milling time in the diffractogram patterns. Results indicates that milling time and NbC addition improves the milling efficiency significantly and being possible to obtain nanoparticles.

Keywords: *aluminum bronze; niobium carbide; high energy ball milling; powder metallurgy*

1. Introduction

The aluminum bronze alloy is useful in a great number of engineering structures with applications in different industries as aerospace and shipbuilding. Among the copper alloys, aluminum bronzes are used extensively because they possess superior properties such as high strength, oxidation and corrosion resistance in marine environment, wear, cavitation and impact resistance¹⁻⁴. Most categories of aluminum bronze contain 4-11 wt. % aluminium in addition, that increase the mechanical properties of the alloy establishing a face-centered cubic phase (FCC), which improves the casting properties and hot working of the alloy. Other alloying agents such as iron, nickel, manganese and silicone may be present in varying proportions. The higher strength of aluminium bronze compared with similar to low alloy steels and other copper alloys and makes it suitable for the production of forgings, plates, sheet, extruded rods and sections⁵⁻⁸.

In conventional metallurgical processes usually no more than 54% of aluminum alloy chips are recovered. However in powder metallurgy process 95% of metal chips can be recovered. The benefits of the direct conversion of aluminum alloy scrap into compact metal include also a possible reduction of energy consume, environment protection and less air pollution emission⁹.

Powder metallurgy (PM) is a highly developed technique for manufacturing composites and processing commonly used

for the fabrication of engineering components and particulate reinforced metal matrix composites. The basic process involved in PM technology route is mixing powder elements, termed mechanical alloying, or milling of metal scraps and uniform composition powders, termed mechanical milling, such as pure metals, intermetallics, or prealloyed powders, to the compacting those powder elements in a die at room temperature and the sintering the consolidated powders for densification. The densification process is generally carried out by conventional methods using a furnace¹⁰⁻¹⁴.

Compared with traditional methods, powder metallurgy (P/M) process has numerous advantages for fabricating small pieces of complicated shapes, because it allows material and energy savings as well as dimensional accuracy¹⁵⁻¹⁶. Moreover, it has better control on the microstructure where better distribution of the reinforcements is possible, and this great influence on the end properties¹⁷⁻¹⁹.

In recent years, extensive work has been undertaken to sinter metal matrix composites which contain ceramic particles embedded in the metal matrix. This class of ceramic material is termed as carbide and has drawn great interest due to exceptional profile of mechanical, physical and chemical properties. Carbides are compounds in which carbon is combined with less electronegative elements of a metal or a semimetal that can improve the properties of material, such as wear resistant, with the addition of particulate metal carbides dispersed in the metal matrix. Carbides have higher hardness, elastic modulus and resistance to wear than high

* e-mail: aottoboni@yahoo.com.br

strength steels. Especially, niobium carbide (NbC) it is a refractory metal and bulk compound that exhibits a hardness beyond 20 GPa, good chemical properties, elevated Young's modulus and a high melting point above 3000°C²⁰⁻²².

Demand for niobium has increased significantly over the last 45 years, particularly as a micro-alloying element in high strength and stainless steels. In such alloys, niobium forms a dispersed micro/nanosized particle, controlling the microstructure and thus improving mechanical properties. Most studies have focused on sintering with additions of hard ceramics such as NbC with the aim of producing a more wear resistant composite²³⁻²⁶.

Particle size is also an important factor in PM affecting properties such as compressibility, thus enhancing densification and properties of the sintered products. In this context, high energy ball milling use high energy impacts from the milling balls to repeatedly forge powder particles together which causes a greater reduction of particle size in comparison with traditional milling^{11,15,27}.

This work aimed to study the influence of milling time and carbide addition in the behavior of aluminum bronze alloy during high energy mechanical milling by powder metallurgy route besides characterizing the microstructure and identify of phases. The size reduction of powders is an important factor to improve the properties of diffusion in the sintering process and, consequently, increase the mechanical strength of sintered material in order to make this new composite an alternative for the manufacture of components for aeronautical and naval industries.

2. Materials and Methods

The material studied in this research was the aluminum bronze alloy with following chemical composition: 78.5% Cu; 10.5% Al; 5.1% Ni; 4.8% Fe, similar to the UNS C63020 alloy. In the present study the raw material was obtained in form of chips through the step of machining at slow speed and without the use of lubricants to avoid oxygen and oil-soluble contamination.

The larger chips were broken in small pieces of approximately 10 mm. It was weighted 30 g of these chips and placed with 3% of NbC and 1% of stearic acid in addition (table 1) into stainless steel jar for milling with 300 g of spheres of three different diameters with the same proportion: large with 21 mm, medium with 13 mm and small with 8 mm. The milling was realized using a planetary ball mill for 100 hours in inert argon atmosphere to avoid oxidation of the powders at a milling speed of 300 rpm and a mass/sphere relationship of 1:10. Every 10 hours a sample of milled powder was taken for characterization, however in this work five milling times were chosen to analyze: 10, 30, 50, 70 and 100 hours.

The characterization of the aluminum bronze milled powder was realized using a scanning electron microscope Carl Zeiss EVO MA15. In the secondary electron (SE) mode,

Table 1. Mixtures composition for milling process.

Samples	Milling time (h)	Aluminum Bronze weight (g)	NbC weight (g)	Stearic acid weight (g)
1	10	30.0018	0.9061	0.3040
2	30	30.0500	0.9067	0.3046
3	50	30.0070	0.9035	0.3030
4	70	30.0120	0.9012	0.3012
5	100	30.0480	0.9080	0.3078

the particle size variation and morphology of powder were analyzed. Using the back scatter electron (BSD) and energy dispersive x-ray (EDS and Mapping) modes the distribution of NbC produced by Hermann C. Starck company in matrix was evaluated. Particle size distribution was performed in a Microtrac Bluewave S3500 equipment to analyse size of powder with increasing milling time. A X-ray diffraction Panalytical X'pert PRO with CoK_α radiation was used for phase identification with sweeping angle of 30° to 90°, step-size of 0.02° and counting time per step of 1 second.

3. Results and Discussion

The characterization of NbC is shown in Figure 1. In this figure it is possible to note that there are agglomerates with an average size of 20 μm composed of small particles upon larger particles and smaller particles with near of nanometer sizes.

SEM image of milled aluminum bronze is shown in Figure 2 to 6. It is possible to observe that 10 hours of milling chips from the machining process were not sufficient for the formation of particles or material powder and the chip size shown in Figure 2 and has a larger size than 1000 μm. The chip of aluminum bronze maintained its morphology and dimension in comparison with the chip before the milling process. The energy of 10 hours of milling was not sufficient to achieve the shear of chips. As the aluminum bronze has a face-centered cubic (FCC) crystalline structure, due to the

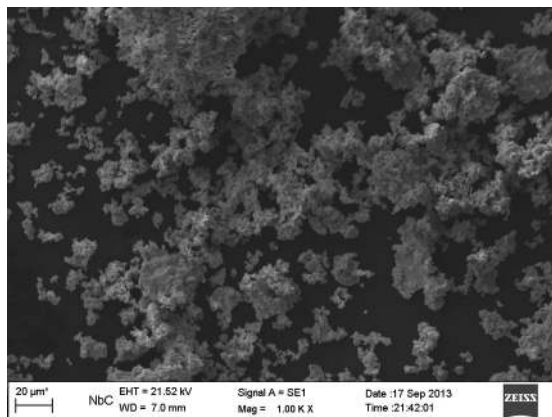


Figure 1. NbC powder.

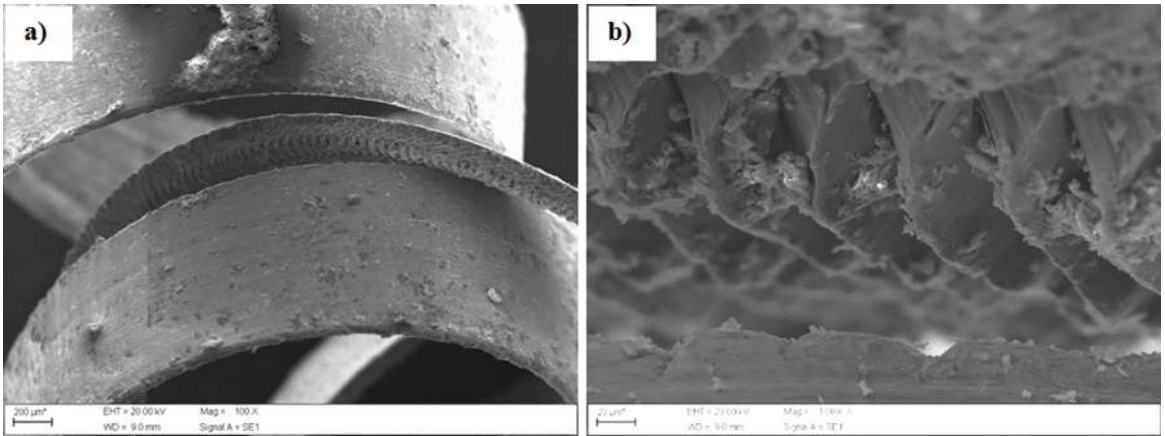


Figure 2. Morphology of the aluminum bronze chip milled for 10 hour (a); sheared surface morphology of one of chip in detail (b).

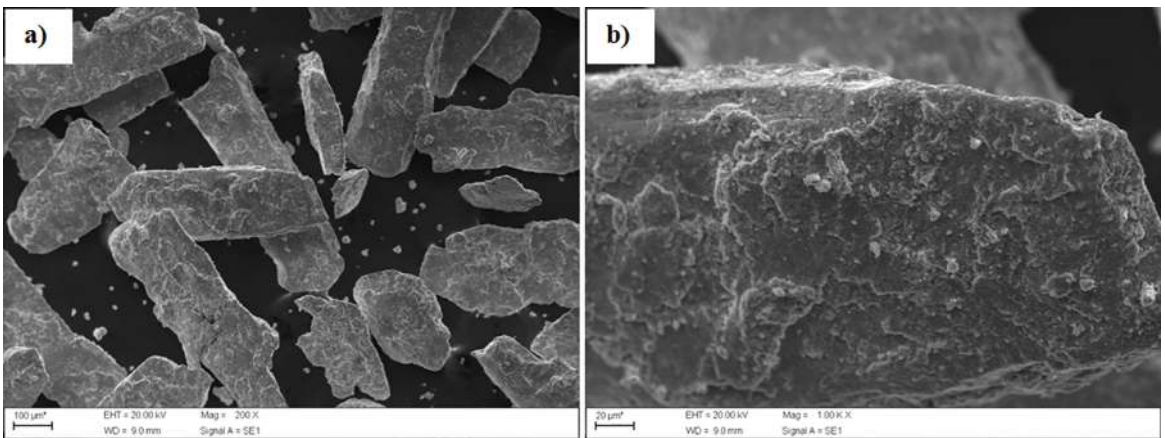


Figure 3. Aluminum bronze milled for 30 hours in rod shaped (a); lump of one particle (b).

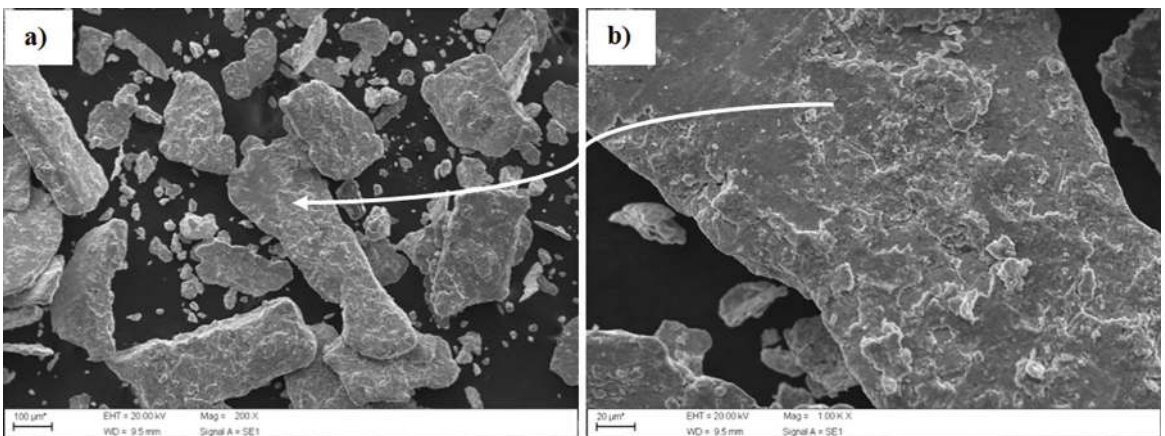


Figure 4. Aluminum bronze alloy milled for 50 hours beginning a spherical shape (a); morphology of lump produced (b).

greater number of crystal planes in its structure, there is a chance of slipping these planes, which reduces the possibility of strain hardening of this material.

It can be observed in Figure 3 that after 30 hours of milling, the chip of the aluminum bronze modified its morphology and dimension in comparison with the chip

milled by 10 hours (Figure 2). With increase the milling time to 30 hours, the chips of the aluminum bronze alloy were transformed in particles with irregular morphology tending to rod shaped and size around 400 µm.

It was observed that with increase in the milling time from 30 hours to 50 hours particle size get reduced (Figure

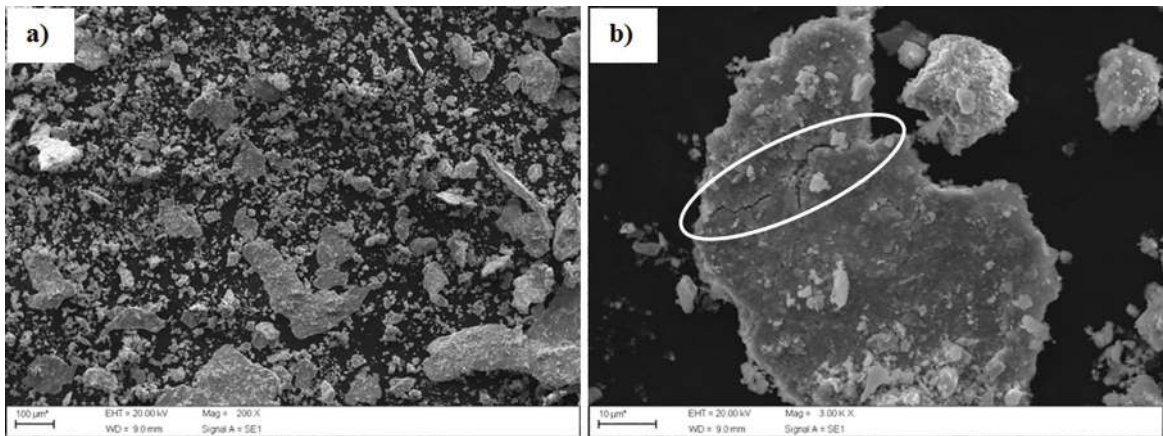


Figure 5. Aluminum bronze alloy milled for 70 hours in form of powders (a); particle fracture due to the milling process (b).

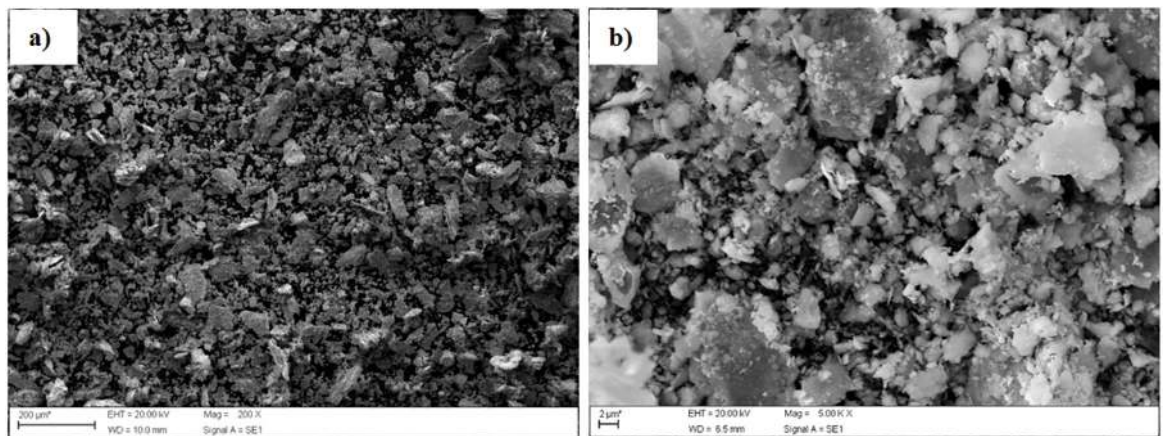


Figure 6. Aluminum bronze powders after 100 hours milling (a); morphology of different submicrometric particles (b).

4). However, it can be seen that the particles are beginning to get spherical shape although there are still larger and irregular particles with sizes around 300 µm. The arrow in the Figure 4 represents the shear surface of the particles caused by deformation and consequent displacement of crystal planes during collisions between particles in the milling process.

When the milling of the aluminum bronze reaches 70 hours (Figure 5) it was observed that there are still particles with sizes of 100 µm, but also a high amount was broken in small particles having size 10 µm. The encircled region in Figure shows the shear area of a particle.

A major homogeneity was observed in Figure 6 with 100 hours of milling. It can be observed a significant reduction in the obtained particles, demonstrating an increase in the milling process efficiency. Most particles have size of 10 µm and the presence of nanoparticles it can be seen too. This condition proves that milling time is a very important parameter to milling process achieve smaller particles sizes and especially nanometric sizes.

The carbide distribution was evaluated under the scanning electron microscope (SEM) using the energy dispersive

x-ray (EDS) mode and mapping analysis (Figure 7). It was observed that the NbC particles were located homogeneously on the surface of the aluminum bronze particles milled at 100 hours. The NbC particles were identified by its chemical elements Carbon and Niobium. In Figure 7a the alloy it's analysed using the back scatter electron (BSD) mode where the brighter spots represent the niobium because of its higher atomic weight. The Figure 7b represents the distribution of Nb and C in the matrix where the green stains represent the C element and red stains represent the Nb element.

From the EDS analysis in Figure 8, it is possible to observe the presence of main elements that compose the aluminum bronze alloy as Cu, Al, Fe and Ni, although it is not possible to say whether the Fe and Ni are derived exclusively of material or are part of a contamination of stainless steel jar used in the milling, differently of Cr presence that certainly is a contamination of the jar. Already the elements Nb and C are part of niobium carbide added in the mixture.

The results of the particle size analysis are shown in Figure 9. It is possible to note that milling time and niobium carbide addition exert great influence in breaking

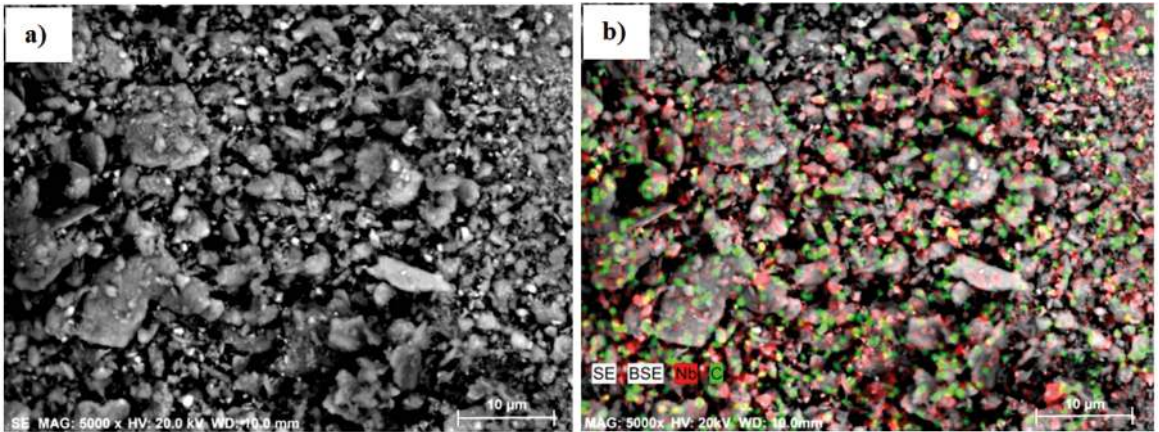


Figure 7. SEM image of aluminum bronze particles after 100 hours in the BSD mode (a); mapping analysis for NbC particulate identification (b).

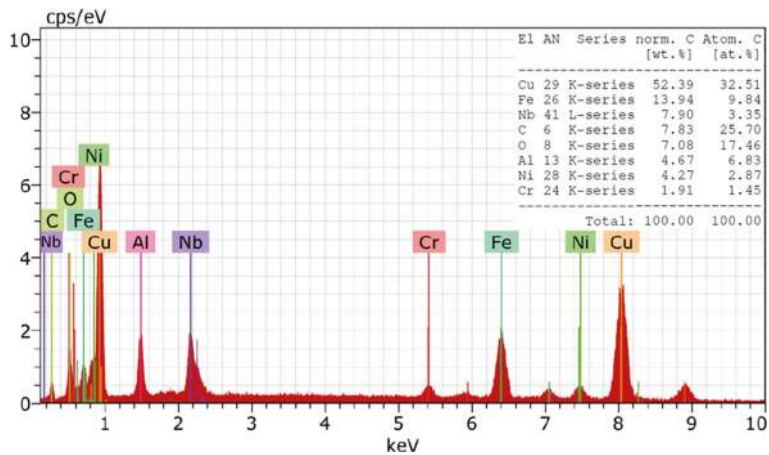


Figure 8. EDS analysis of aluminum bronze for identification of main chemical elements.

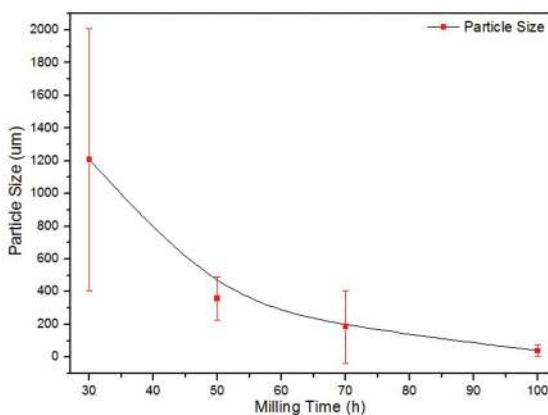


Figure 9. Particle size analysis in function of milling time.

of chips and subsequent size reduction of aluminum bronze particles, which is considered ductile material. The particle size distribution analysis were performed after 30 hours of milling, since 10 hours the material further presented in the form of chip. Thus, at 30 hours, the material still

has large particle size around 1200 μm. With 50 hours, material shows significantly lower mean particle size of 350 μm due to high energy collisions and the combination of milling factors time and NbC addition. Already with 70 hours, the material presents size below 200 μm, where there is a high shear rate the particles caused by the shock of hard particles of NbC. Finally, with 100 hours, the aluminum bronze powder reaches its smaller size around 30 μm due precisely to the formation of a ductile-fragile particle system and high milling time.

The cumulative particle size analysis curve seen in Figure 10 shows the limits of D10, D50, and D90 used as the acceptance criteria for the laser diffraction method. For example, according of values provided by the equipment, it can be noted in the graph that for 100 hours milling D50 is 39.43 μm, which represents 50% of particle sizes are below this value (i.e., the median diameter). Similarly D10 and D90 are 9.93 μm and 103.5 μm, indicating that 10% of particles are below 9.93 μm and 90% of particles are below 103.5 μm respectively.

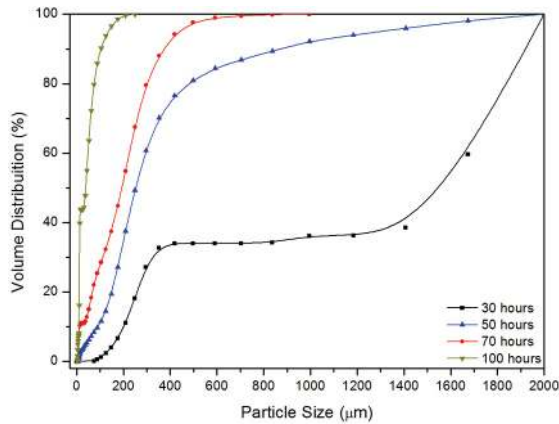


Figure 10. Cumulative particle size distribution.

It can be seen in Table 2 the “D” values referring to D10, D50, and D90 of the aluminum bronze powders in function of milling time.

Table 2. Aluminum bronze powders “D” values.

Milling time (h)	D10 value (µm)	D50 value (µm)	D90 Value (µm)
30	202.2	1580	1887
50	90.47	251.5	866.2
70	12.71	193.8	369.3
100	9.93	39.43	103.5

The different phases of aluminum bronze are shown in Figure 11 and were identified with the aid of X-ray diffraction. The XRD patterns were added using the ICSD Crystalline Structures Base for principal α phase and intermetallics κ phases.

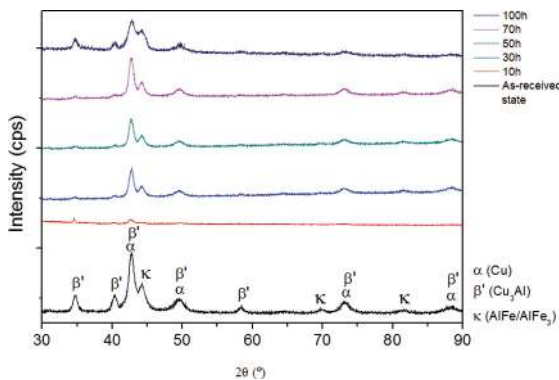


Figure 11. X-ray diffraction and phases of aluminium bronze.

Amounts of β' metastable phase were found through the comparison with other studies of XRD²⁸. The presence of metastable β' phase in aluminum bronze, termed martensite, is due to preliminar heat treatment TQ-30 (ASM 4590B) that alloy fused receive in aerospace applications in order to increase mechanical properties as tensile strength and hardness²⁹.

It can be noted in diffractogram of Figure 12 that peak intensity decreases and its width grows as the milling time increases and the material is moving toward their amorphization due to introduce of mechanical deformation in the crystalline planes resulting in particle and crystallite refinement. This fact can be confirmed by enlargement and until the disappearance of the characteristic peaks of the material in the as-received state when compared with the material subjected to milling times of 10 to 100 hours.

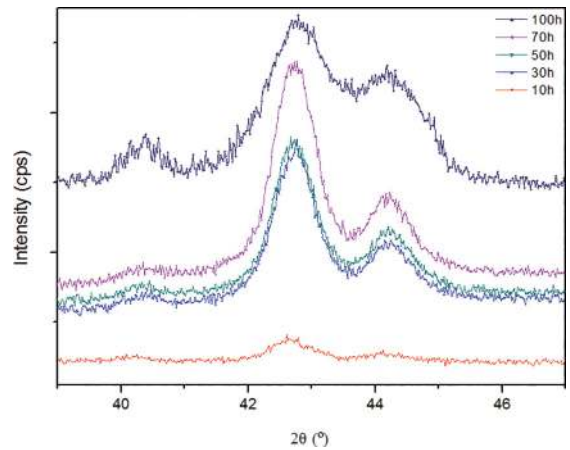


Figure 12. XRD spectra of aluminium bronze peak widening after milling.

The peak displacement is related to the deformation of the crystalline structure, which is due to dissolving elements and introduction of defects as substitutional impurities during milling process modifying the lattice parameter. On milling for 10 h, aluminum bronze has no peaks because at this time the material is still in form of chips. Due to their irregular shape the X-rays reflection incident on the material, and consequently on the crystal planes, is disordered causing the XRD detector can not correctly receive those x-rays to make a diffractogram correctly. The continued milling for 30 h, 50 h, 70 h and 100 h where the powder started losing crystallinity with the enlargement of the peaks and decrease of intensity, indicative of beginning of an amorphous phase.

4. Conclusions

From the use of high energy ball milling process, it was possible to obtain powders of the aluminum bronze from chips of material in various milling times. The parameter time was crucial and contributed to reducing the size of the material, as seen in the D50 values beginning in 1580 µm to particles of 39.43 µm.

The evolution of the milling process efficiency producing ever smaller particles can be observed both in the SEM images as in particle size analysis. It was observed also that with NbC additions there was a significant increment in the

milling efficiency, which enables the obtainment powders in nanometric scale.

The XRD analysis shown various phases which compose the aluminum bronze as important β' phase that represents metastable martensite that increase its mechanical resistance. The presence of nanoparticles in the aluminum bronze subjected at 100 hours milling can improve some properties of powders after sintering process as density and porosity giving a more resistant material.

5. Acknowledgements

This work was financially supported by CAPES. We would also like to thank the UNIFEI characterization's laboratory for the technical support.

6. References

- Copper Development Association. *Aluminum Bronze Alloys for Industry*. CDA Publication. 1986;83. Available from: <<http://copperalliance.org.uk/docs/librariesprovider5/resources/pub-83-al-bronze-alloys-for-industry-pdf.pdf?Status=Master&sfvrsn=0>>. Access in: 22/3/2017.
- Su Y, Liu G, Wu D, Liu Z. The research of corrosion resistance of aluminum-bronze surfacing layer. In: *Proceedings of the 2nd International Conference on Electronic & Mechanical Engineering and Information Technology (EMEIT-2012)*; 2012 Sep 9-12; Shenyang, Liaoning, China. Paris: Atlantis Press; 2012. p. 1495-1498.
- Al-Hashem A, Riad W. The role of microstructure of nickel-aluminium-bronze alloy on its cavitation corrosion behavior in natural seawater. *Materials Characterization*. 2002;48(1):37-41.
- Shivraman T, Dwivedi DK. Microstructure evolution and tribological behavior of the solid lubricant based surface composite of cast nickel aluminum bronze developed by friction stir processing. *Journal of Materials Processing Technology*. 2016;238:30-38.
- Pisarek BP. The crystallization of the aluminium bronze with additions of Si, Cr, Mo and/or W. *Archives of Materials Science and Engineering*. 2007;28(8):461-466.
- Sekunowo OI, Adeosun SO, Lawal GI, Balogun SA. Mechanical Characterisation of Aluminium Bronze-Iron Granules Composite. *International Journal of Scientific & Technology Research*. 2013;2(4):179-185.
- Derek ET, William TB. Introduction to copper and copper alloys. In: *ASM Handbook Volume 2: Properties and Selection: Nonferrous Alloys and Special-Purpose Materials*. 10th ed. Materials Park: ASM International; 1990.
- Kear G, Barker BD, Stokes KR, Walsh FC. Electrochemistry of non-age 90-10 copper-nickel alloy (UNS C70610) as a function of fluid flow. Part 2: Cyclic voltammetry and characterisation of the corrosion mechanism. *Electrochimica Acta*. 2007;52(7):2343-2351.
- Gronostajski J, Chmura W, Gronostajski Z. Phases created during diffusion bonding of aluminium and aluminium bronze chips. *Journal of Achievements in Materials and Manufacturing Engineering*. 2006;29(1):32-37.
- Totten GE, ed. *Steel Heat Treatment: Metallurgy and Technologies*. Boca Raton: CRC Press; 2006.
- Dhanasekaran S, Gnanamoorthy R. Abrasive wear behavior of sintered steels prepared with MoS₂ addition. *Wear*. 2007;262(5-6):617-623.
- Suryanarayana C. Mechanical alloying and milling. *Progress in Materials Science*. 2001;46(1-2):1-184.
- Anklekar RM, Bauer K, Agrawal DK, Roy R. Improved mechanical properties and microstructural development of microwave sintered copper and nickel steel PM parts. *Powder Metallurgy*. 2005;48(1):39-45.
- Nawathe S, Wong WLE, Gupta M. Using microwaves to synthesize pure aluminum and metastable Al/Cu nanocomposites with superior properties. *Journal of Materials Processing Technology*. 2009;209(10):4890-4895.
- Kurgan N, Varol R. Mechanical properties of P/M 316L stainless steel materials. *Powder Technology*. 2010;201(3):242-247.
- Ertugrul O, Park HS, Onel K, Willert-Porada M. Effect of particle size and heating rate in microwave sintering of 316L stainless steel. *Powder Technology*. 2014;253:703-709.
- Rahimian M, Ehsan N, Parvin N. The effect of particle size, sintering temperature and sintering time on the properties of Al-Al₂O₃ composites, made by powder metallurgy. *Journal of Materials Processing Technology*. 2009;209(14):5387-5393.
- Oghbaei M, Mirzaee O. Microwave versus conventional sintering: A review of fundamentals, advantages and applications. *Journal of Alloys and Compounds*. 2010;949(1-2):175-189.
- Zheng RR, Wu Y, Liao SL, Wang WY, Wang WB, Wang AH. Microstructure and mechanical properties of Al/(Ti,W)C composites prepared by microwave sintering. *Journal of Alloys and Compounds*. 2014;590:168-175.
- Aldinger F, Uchino K, Koumoto K, Kaneno M, Spriggs RM, Somiya S, eds. *Handbook of Advanced Ceramics: Materials, Applications, Processing and Properties*. San Diego: Academic Press; 2003.
- Madej M. Phase reactions during sintering of M3/2 based composites with WC additions. *Archives of Metallurgy and Materials*. 2013;58(3):703-708.
- Subramanian C, Stratford KN, Wilks TP, Ward LP. On the design of coating systems: Metallurgical and other considerations. *Journal of Materials Processing Technology*. 1996;56(1-4):385-397.
- Woydt M, Mohrbacher H. Friction and wear of binderless niobium carbide. *Wear*. 2013;306(1-2):126-130.
- Woydt M, Mohrbacher H. The tribological and mechanical properties of niobium carbides (NbC) bonded with cobalt or Fe₃Al. *Wear*. 2014;321:1-7.

25. Mohrbacher H, Zhai Q. Niobium Alloying in Grey Cast Iron for Vehicle Brake Discs. In: *Proceedings of Materials Science & Technology Conference and Exhibition 2011*; 2011 Oct 16-20; Columbus, OH, USA. Materials Park: ASM International. p. 434-445.
26. Acchar W, Camara CRF, Cairo CAA, Filgueira M. Mechanical performance of alumina reinforced with NbC, TiC and WC. *Materials Research*. 2012;15(6):821-824.
27. Klar E, Samal PK. *Powder Metallurgy Stainless Steels: Processing, Microstructures, and Properties*. Materials Park: ASM International; 2007. 256 p.
28. Cenoz I. Metallography of aluminum bronze alloy as cast in permanente iron die. *Metallurgical & Materials Engineering*. 2010;16(2):115-122.
29. Rodrigues CA, Melo MLNM, Paes LES. Caracterização de uma liga de bronze de alumínio submetida a diferentes tratamentos térmicos. *Rem: Revista Escola de Minas*. 2012;65(3):343-348.